Spring 2013

The inner workings of the DNA copying nanomachine : kinetic studies of DNA polymerase I from the thermophilic bacterium Rhodothermus marinus

Emily P. Kornberg
University of Richmond

The Inner Workings of the DNA Copying Nanomachine: Kinetic Studies of DNA Polymerase I from the thermophilic bacterium *Rhodothermus marinus*

Presented By

Emily P. Kornberg

Honors Thesis in the Department of Biochemistry and Molecular Biology

May 2013

University of Richmond

University of Richmond, VA 23173

This honors thesis fulfills all requirements as enumerated by the Honors Program in Biochemistry and Molecular Biology at the University of Richmond.

Advisor signature — *date* 4/26/13

Reader signature — *date* 4/26/13

Department signature — *date* 4/26/13

ABSTRACT

DNA polymerase I from *Rhodothermus marinus* is a high-fidelity DNA polymerase capable of operating at high temperatures and incorporating 2´,3´-dideoxynucleotides. The *R. marinus* DNA Polymerase I active site contains an unusual proline in the middle of a mobile "O helix." This proline residue is hypothesized to decrease the relative free energy of a kinetic checkpoint termed the ajar conformation, and thereby slow the incorporation of incorrect nucleotides. We aim to test the accuracy of a newly developed nucleotide incorporation model, in which the enzyme allows the template to interact with the bound dNTP in the ajar conformation, whether correct or incorrect, prior to catalyzing phosphodiester bond formation. The active site proline 760 in *R. marinus* DNA Pol I was mutated and error rates were determined to test this new model of nucleotide selection. Our studies have further characterized a "missing link" in the mechanism for nucleotide discrimination in high-fidelity DNA polymerases.

INTRODUCTION

DNA synthesis is a vital chemical reaction in biology because it is the mechanism by which genetic material is copied and passed from one cell to another. This process is remarkably fast and accurate, with nucleotide addition rates of tens or hundreds of nucleotides per second and error rates between one error per ten thousand to one million nucleotides copied for replicative polymerases [1]. The high fidelity of DNA polymerases is achieved by employing a complex induced-fit mechanism wherein the enzyme encloses around a complementary incoming deoxynucleoside triphosphate (dNTP) and aligns the 3´-hydroxyl of the growing DNA strand to the α-phosphate of the dNTP for in-line attack [2]. Mismatches are misaligned in the polymerase active site, leading to slower incorporation and dissociation [3].

Once the dNTP is bound, the enzyme transitions from an "open" to a "closed" conformation, which encloses the free nucleotide opposite the base on the template DNA. During this conformational change, a dislocation of a conserved tyrosine in the "O helix" enables the template nucleotide to pair with the free dNTP in the newly formed "insertion site" (Figure 1). Based on existing data, it is evident that DNA polymerase adopts the same conformation for all four of the possible dNTPs and does not distinguish one base from another. Because of this, the enzyme must allow the template base to preview all four of the dNTPs individually in order to distinguish between the correct and incorrect dNTP match [8].

Many DNA polymerases also contain the ability to proofread their own work through an attached 3´-to-5´ exonuclease domain. As the polymerase processively synthesizes DNA, occasional errors occur and slow the rate of synthesis due to misalignment of substrates and active site residues. Mismatched nucleotides in the growing DNA strand can then be transferred to the 3´-to-5´ exonuclease active site, which cleaves 3´-terminal nucleotides using a two-metal-

ion catalytic mechanism [4,5]. The enzyme can then resynthesize the DNA, resulting in higher fidelity for DNA synthesis. Proofreading improves fidelity by up to two orders of magnitude [1].

In addition to their essential roles in all life forms, DNA polymerases also have important functions in the laboratory setting. Technologies such as polymerase chain reaction and DNA sequencing are essential and transformative to biology and biotechnology and have been developed based on knowledge of DNA polymerase function. DNA polymerases from thermophilic organisms have been particularly useful for biotechnology, allowing reactions to be performed at high temperatures [8]. The *R. marinus* DNA polymerase I contains a proline in place of a highly conserved valine or isoleucine in the polymerase O helix (Figure 2), which prevents the O helix from its normal functional flexibility. This proline "wedge" may play a key role in the accuracy of the polymerase through the stabilization of the previously described ajar conformation [8]. This conformation falls between the open and closed conformations adopted by the polymerase in which the O helix subdomain reaches an intermediate point in its movement, allowing the incoming dNTP to be matched against the template DNA strand and identified as a correct or incorrect match.

Previous studies conducted on DNA Polymerase I from another bacterium *Bacillus stearothermophilus* have indicated that the polymerase adopts a previously characterized ajar conformation prior to the closed conformation that allows the polymerase to incorporate nucleotides into the growing DNA strand with more accurately, yet more slowly [8]. In studies conducted by Wu *et. al.* [8] a valine residue at position 713, the hinge of the O helix that allows for its flexibility when incorporating nucleotides, was mutated to a proline (Figure 3). Kinetics studies showed a slowed rate of incorporation of both correct and incorrect nucleotide bases,

which suggests that the transition from the ajar to the closed conformation is indeed part of the enzyme mechanism.

We hypothesize that the *R*. marinus DNA polymerase I enzyme will more readily form the ajar conformation in the presence of nucleotides due to having a proline "wedge" in the active site, allowing the enzyme to make fewer mismatched nucleotide base pairs and have a higher relative efficiency, which is an indicator of how often the enzyme incorporates incorrectly matched base pairs into the growing DNA strand. To test this hypothesis, we will employ site-directed mutagenesis to remove to the proline wedge from *R. marinus* DNA polymerase I. If the proline wedge serves as a barrier to the closed conformation, as hypothesized in the model, then its removal should speed up the enzyme. We aim to further characterize this conformation by means of kinetics assays using quench flow analysis and capillary electrophoresis imaging to quantify the incorporation of correctly and incorrectly-matched nucleotides by the *R. marinus* 3'-5' exonuclease-domain-deficient polymerase, its mutant with the proline "wedge" in the active site mutated to a valine, and Taq DNA Polymerase I, which has a valine residue at the glycine hinge in the O helix (Figure 3), into a growing DNA strand. These assays provide the information necessary to calculate and compare the *in vitro* error rate of each enzyme used.

MATERIALS AND METHODS

Cloning. DNA fragment encoding the 5'-'3 exonuclease deficient DNA polymerase I from *Rhodothermus marinus* (RF; residues 329-924 plus an N-terminal methionine) was amplified by PCR from genomic DNA (American Type Culture Collection, Manassas, Virginia), and inserted

into pCR2.1-TOPO vector (Invitrogen, Carlsbad, California) as XhoI restriction-enzyme fragment. Oligonucleotides used for amplification were 5´-CATATGGAAAAGGCGGACTACCGGATCGTC-3 ´and 5´-TCAGTGGGCATCCAGCCAGTTGTC-3´. Gene was sequenced using Sanger sequencing and inserted into a bacterial expression vector, pET-21a (Novagen), as a XhoI restriction-enzyme fragment.

Site-Directed Mutagenesis: The D497A mutation was generated using the QuikChange site-directed mutagenesis kit (Stratagene, La Jolla, California) with Phusion High-Fidelity DNA Polymerase (New England Biolabs, Ipswich, Massachusetts). The oligonucletoides used for the D497A and P760V mutagenesis reactions were 5´-CCCTATGCCTGTGAAGCCACGGACATTGCACTG-3´/5´-CAGTGCAATGTCCGTGGCTTCACAGGCATAGGG-3´ and 5´-CCAAGATGGTCAACTACGGCATTGTCTACGGGATTTCGG-3´/5´-CCGAAATCCCGTAGACAATGCCGTAGTTGACCATCTTGG-3´, respectively. The mutations were confirmed by Sanger DNA sequencing using fluorescent terminators (Eurofins MWG Operon, Huntsville, Alabama).

Protein expression and purification. The pET-21a plasmid containing the RF gene with the D497A mutation was transformed into *Escherichia coli* BL21(DE3) cells (Lucigen, Middleton, WI). Native D497A RF protein was produced using standard overexpression techniques. Inoculated 500 mL LB/Amp Media with 20 mL overnight culture and grew at 37 °C to OD_{600}=0.600. Expression of protein was induced with IPTG (4 mM) and the cells were incubated overnight at 37°C. Cells were harvested by centrifugation at ~3000Xg for 15 minutes, and stored at 4 °C.

A bacterial pellet from cell culture was resuspended and lysed in B-PER (Bacterial Protein Extraction Reagent 20 mM Tris Buffer, pH 7.5; Thermo Fisher Scientific, Rockford, Illinois). Lysate was centrifuged at ~7500Xg for 30 minutes and supernatant was heated in 65 °C water bath for 20 minutes. Lysates were centrifuged again at 7500 RPM for 30 minutes, and supernatant containing heat-stable proteins was dialyzed in 1x Buffer A (50 mM Tris-HCl pH 7.5, 1 mM ethylenediamine tetraacetic acid, 6.5 mM 2-mercaptoethanol). Supernatant was passed through heparin sepharose column equilibrated in 1x Buffer A using a linear gradient containing 1x Buffer A and 50% 1x Buffer A & 1.5 M sodium chloride (Buffer B). Fractions containing the protein were collected and exchanged back into 1x Buffer A through dialysis. The fractions were then passed through S1 ion exchange column (BioRad) pre-equlibrated with 1x Buffer A using a linear gradient containing 1x Buffer A and 1x Buffer B. Fractions containing protein were combined and concentrated using 10 kDa Amicon centrifugal concentrators (EMD Millipore). Protein sample was run through S1 ion-exchange column again to remove remaining impurities, again using linear gradient of 1x Buffer A and 1x Buffer B. Fractions containing RF were exchanged into 1x Buffer A through three cycles of concentration and dilution, and concentrated to 1 mL in 50 kDa Amicon centrifugal concentrator.

Kinetics Assays and data collection. Complementary oligonucleotides used in the solution studies were synthesized by Operon Biotechnologies, Inc. (Huntsville, AL). The template (5'-TTACTTGACCAGATACACTGTCTTTGACACGTTGATGGATTAGAGCAATCACATCCAAGACTGGCTATGCACGAA-3') and fluorescently labeled primer (5'-6-carboxyfluorescein-TCGTGCATAGCCAGTCTTGGATGTGATTGCTCTAATCCATCAACGTGTCAAAGACAGTGTATCTGGT-3') strands were annealed as described [18] (Figure 4). The DNA substrate and

wild type, P760V, or Taq DNA Polymerase I proteins were diluted with reaction buffer (50 mM Tris-HCl, pH 8.0, 50 mM NaCl, 10 mM MgCl2, 1 mM DTT) to 0.1 and 2 μM, respectively. RF-DNA or Taq-DNA complexes were mixed with equal volumes at various concentrations of dCTP or dTTP. The reaction (50°C) was quenched at different time points using four reaction volumes of quench solution (95% formamide (v/v), 25 mM EDTA). Reactions slower than 1000 ms (RF-dTTP) were executed manually. Reactions faster than 1000 ms (RF-dCTP) were executed using a KinTek RQF-3 Rapid Quench Flow instrument (KinTek Corp., Austin, TX). Primer extension was quantified by capillary electrophoresis with fluorescence detection, using an ABI3100 Genetic Analyzer (Applied Biosystems, Foster City, CA). Pre-steady-state kinetic constants were determined and fit as described using KaleidaGraph (Synergy Software) [8].

RESULTS

Bacterial DNA polymerase I enzymes contain an N-terminal 5´-to-3´ exonuclease domain, a central 3´-to-5´ exonuclease domain for proofreading, and a C-terminal polymerase domain. The N-terminal 5´-to-3´ exonuclease domain has been shown to be dispensable for the DNA synthesizing activity of several DNA polymerases, including DNA polymerase I from *Escherichia coli* (Klenow fragment), *Thermus aquaticus* (Klentaq1), and *R. marinus*[9-12]. Due to the improved stability of the N-terminal truncated protein [9], we chose to express the large fragment (amino acids 329-924) of the *R. marinus* DNA polymerase I, which we term "Rhodothermus fragment", or RF.

Site-directed mutagenesis was utilized to inactivate the 3´-to-5´ exonuclease domain of RF for kinetic studies and future co-crystallization trials with DNA. An active nuclease activity could potentially digest the DNA in complex with the enzyme, therefore not allowing for an accurate measurement of nucleotide incorporation. The 3´-to-5´ exonuclease domain of DNA polymerase I from *R. marinus* shares strong homology to the *E. coli* exonuclease domain and is active [9], as opposed to the inactive domains of DNA polymerases from other thermophiles, *Bacillus stearothermophilus* [13] and *Thermus aquaticus* which do not have a fully developed active site to support this exonuclease activity. [14,15] All four acidic residues that bind two divalent cations in the 3´-to-5´ exonuclease domain [4] are conserved. The single mutation that decreases exonuclease activity the most in *E. coli* DNA polymerase I is aspartic acid 501 to alanine (D424A) [5]; thus we made the equivalent mutation, D497A, in RF to inactivate its exonuclease activity.

Site-directed mutagenesis was again utilized to mutate a proline at position 760 in RF to a valine. By removing this proline "wedge" at the hinge of the O helix, the enzyme without this stabilized ajar conformation can be analyzed by monitoring its rate of incorporation of nucleotides and the subsequent relative efficiency of the enzyme.

Kinetics Assays

RF, the P760V mutant, and Taq DNA Polymerase I were allowed to incorporate a single nucleotide into a template strand 5'-deoxyguanosine overhang on a 6-FAM tagged template and primer DNA complex (Figure 6). Quench flow assays were conducted via mixing our enzyme (2 μM)-DNA (.1 μM) complex with either deoxycytosine triphosphate (dCTP) or deoxythymine triphosphate (dTTP) nucleotide at various concentrations (0.005-0.1 mM and 0.025-1.0 mM,

respectively) and quenching the reaction with Formamide and EDTA after a specified amount of time (10-1000 ms and 20-3000 sec, respectively). A broad range of concentrations for each nucleotide was used in order to acquire the most accurate constants for each enzyme. Each sample was shipped to Dr. Scott Langdon at the Duke DNA Analysis Facility for capillary electrophoresis analysis (Figure 4). Using this data the amount of extension of the primer DNA strand could be quantified, and the fraction of primer extension could be plotted against time for each concentration of nucleotide used in experiments (Figure 5). Initial rates of incorporation could be derived from these plots and, using Michaelis-Menten kinetics, the k_{pol}, K_D, and relative efficiency could be determined for each enzyme. Each of these constants were calculated and the results are reported in Table 1. Also included with the acquired data are the results from previous studies using *Bacillus* fragment (BF).

DISCUSSION

From existing structural data [16], it is clear that DNA polymerase adopts the same open conformation for all four template bases and does not distinguish one template base from another. Thus, the enzyme, because it is capable of incorporating all four dNTPs, must allow the template to preview all four nucleotides individually in order to distinguish between the correct and incorrect dNTP. Therefore, there must exist a conformation in which the enzyme allows the template to interact with the bound dNTP, whether correct or incorrect, before phosphodiester bond formation is catalyzed [17]. Previous structural studies have revealed a new conformation in which the template base forms a base pair with the incoming nucleotide, but the enzyme does not

proceed to the closed conformation. Rather, the O helix adopts a conformation intermediate of the open and closed conformations, which has been termed the "ajar" conformation. This ajar conformation is made possible by a glycine hinge in that last turn of the O helix (Figure 3), where the O helix bends sharply. The enzyme used in these previous experiments was mutated such that a valine at position 713, in the hinge of the O helix, was replaced by a bulky proline residue [8]. This V713P mutant enzyme showed slower nucleotide incorporation rates for both complementary pairs and mismatches, suggesting that the transition from ajar to closed conformations is an important step in the polymerase mechanism. The V713P mutation actually slowed G:T mismatch incorporation more than complementary G:C nucleotide addition, in turn making the enzyme more accurate. Using these data, a new model for nucleotide selection in DNA polymerase I enzymes was formulated. In this model (Figure 2), DNA polymerase I uses the ajar conformation as a preview conformation to check the nucleotide for Watson-Crick base pairing with the template. Good matches advance to the closed conformation [8]. The ability to adopt the ajar conformation is a critical part of the mechanism to distinguish mismatches.

Through our experiments with RF, we have further supported this model by altering the ajar conformation in another DNA polymerase and measuring the enzyme fidelity. The presence of proline 760 in the active site of RF DNA Polymerase I made possible the inverse experiment of that with BF. We hypothesized that the mutation of proline 760 to valine in RF will remove an energy barrier in the transition from the ajar to closed conformation, increase the rate of catalysis for both correct and incorrect nucleotides, and also decrease the fidelity of the enzyme. Based on the data reported in Table 1, it is clear that rates of catalysis in this mutant RF did in fact increase for mismatched base pair incorporation. The rates of catalysis, however, for complementary matches in the wild type and mutant RF enzymes were not statistically different, and our

hypothesis was not supported in this respect. The mutant RF had a substantially increased G:T mismatch incorporation rate than that of the wild-type RF, suggesting that this stabilized ajar conformation in the wild type RF enzyme plays a critical role in the high-fidelity of the enzyme. Pre-steady state kinetics assays were also performed with Taq DNA Polymerase I in order to provide a frame of reference for our results because this polymerase does not have a proline in an equivalent position in the active site (Figure 3). RF wild-type turned out to be much more accurate than Taq DNA Polymerase I, owing to the location of the proline 760 "wedge" in the active site of the polymerase. Further supporting this observation was the observation that Taq DNA Polymerase I had a higher rate of catalysis for the incorporation of mismatched base pairs compared to the wild type RF enzyme. Data from previous experiments with BF is also included in Table 1 [8]. Comparing the data between the wild type and mutant BF, there is an order of magnitude difference in the incorporation of both complementary and mismatched nucleotides between the two BF enzymes. As previously stated, we found no statistical difference in the k_{pol} for incorporating complementary nucleotides between our wild type and mutant RF enzymes. However, as also seen with BF, we did see an order of magnitude change in the k_{pol} for the incorporation of mismatched nucleotides when comparing our wild type to our mutant RF enzymes. In BF, the K_D for the mutant enzyme decreased dramatically from that of the wild type enzyme when incorporating mismatched nucleotides, indicating a much stronger affinity, and thus a lower K_D, for the incoming substrate due to the stabilized ajar conformation in the mutant enzyme, which allows for greater interactions between the incoming dNTP and the growing DNA strand. With our RF enzymes, we did not see a similar change in affinity for the incorporation of complementary or mismatched nucleotides given the error rates for our K_D values measured for each enzyme. With the stabilization of the ajar conformation in the BF

mutant, the relative efficiency of the enzyme dramatically increased. When we made our backwards mutation in the RF enzyme, in essence de-stabilizing the ajar conformation, we see a dramatic decrease in the enzyme's relative efficiency, thus exhibiting the importance of the role this ajar conformation plays in maintaining the high fidelity of the enzyme.

With these experiments, we have expanded upon the current knowledge in regards to the function of high-fidelity DNA polymerases and further characterized a critical intermediate step in nucleotide incorporation which leads to the high accuracy of these enzymes. These studies and future studies with other polymerases may answer some unresolved questions of how the initial binding of a complementary dNTP encourages the enzyme to move through the initial weak contacts that then develop and increase in strength as the enzyme proceeds to the closed complex. Future studies may also help us understand how the initial weak binding of a mismatched dNTP is recognized by the enzyme and helps it to proceed to a newly characterized ajar conformation, which favors release of the incorrectly matched dNTP over catalysis.

ACKNOWLEDGMENTS

We thank Dr. Scott Langdon and the staff of the Duke University DNA Analysis Facility for their assistance. We thank fellow lab members, Lori Spicer, Brooke Duffany, and Natalie Omattage for assistance with cloning and protein purification.

FIGURE LEGENDS

Figure 1. DNA polymerase I structure preceding phosphodiester bond formation. Complementary nucleotide addition is accompanied by the transition from an open to the closed conformation. This conformational change is characterized by rotation of the O helix in the fingers subdomain, thereby enclosing the correct dNTP within the active site cleft. Reproduced from [8], with permission.

Figure 2. Model for nucleotide sampling and selection. Nucleotides are sampled in the ajar conformation (EA, cyan) and are released if it incorrect, whereupon the enzyme returns to the open conformation (EO, gray), or entrapped in the closed conformation (EC, green) if it is complementary to the template base. Cartoon representations of each state are shown in the center. The red wedge in the hinge of the O helix represents the proline residue at position 760 in RF. Adapted from [8], with permission.

Figure 3. Structure-based manual sequence alignment of nucleotide binding helices of A family DNA polymerases. Phosphate interaction, blue; aromatic residues in the nucleotide binding sites, green; Proposed glycine hinges in the helices; red. BstPolI, EcoPolI, and TaqPolI, DNA polymerase I from *B. stearothermophilus*, *E. coli*, and *T. aquaticus*; hPolG, hPolQ and hPolNu, human DNA polymerases γ, θ, and ν. Reproduced from [8], with permission.

Figure 4. Detection of nucleotide incorporation into a growing primer strand by RF. Capillary electropherograms of primer DNA strand before and after nucleotide addition. The DNA

substrate in Figure 6 was pre-bound to RF and run in an ABI 3100 DNA Analyzer before (A) and after (B) mixing with dCTP. Note the disappearance of the main peak (54.13) and the growth of a new peak (54.87) upon addition of dCTP.

Figure 5. Measuring incorporation of nucleotides as determined by capillary electrophoresis. Each concentration of nucleotide was plotted on a graph with fraction of primer extension on the y-axis and time (s or ms) on the x-axis. Slope of fraction extension plots (m1), or the initial rate of the enzyme in incorporating nucleotides, was used to plot rate (s^{-1}) on the y-axis and concentration (mM) of nucleotide on the x-axis. m1 and m2 values in Michaelis-Menten plots represent k_{pol} and K_D, respectively. Fraction extended and Michaelis-Menten Plot for dTTP incorporation using Taq DNA Polymerase I (A), dCTP incorporation using RF Wild Type (B), dTTP incorporation using RF Wild Type (C), dCTP incorporation using RF P760V (D), dTTP incorporation using RF P760V (E).

Figure 6. 6-FAM-labeled 59-mer primer strand (top) is annealed to a complementary 60-mer template strand, leaving a single G 5'-overhang.

Figure 1.

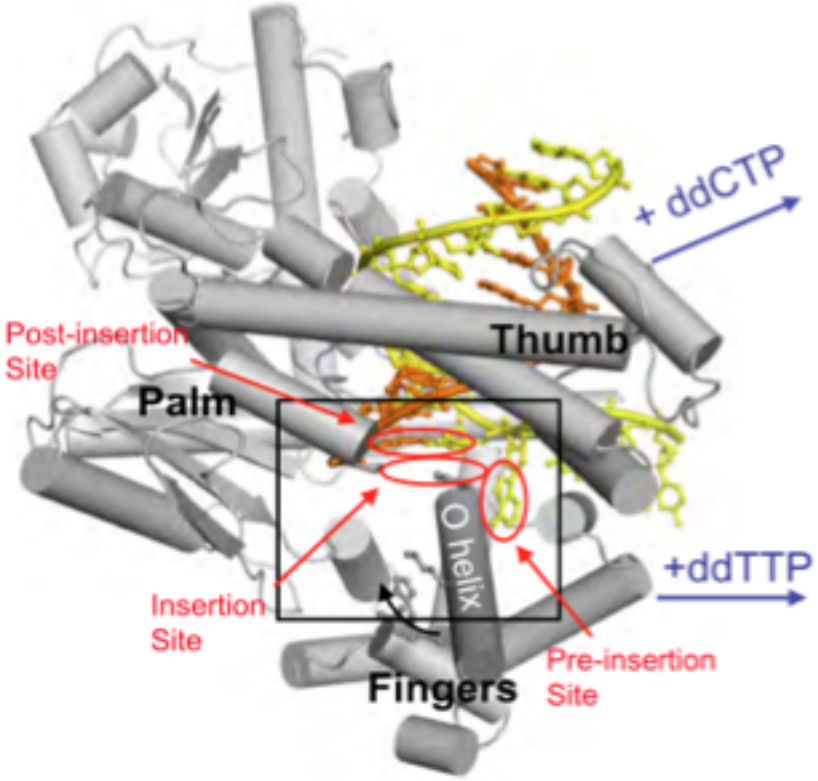

Figure 2.

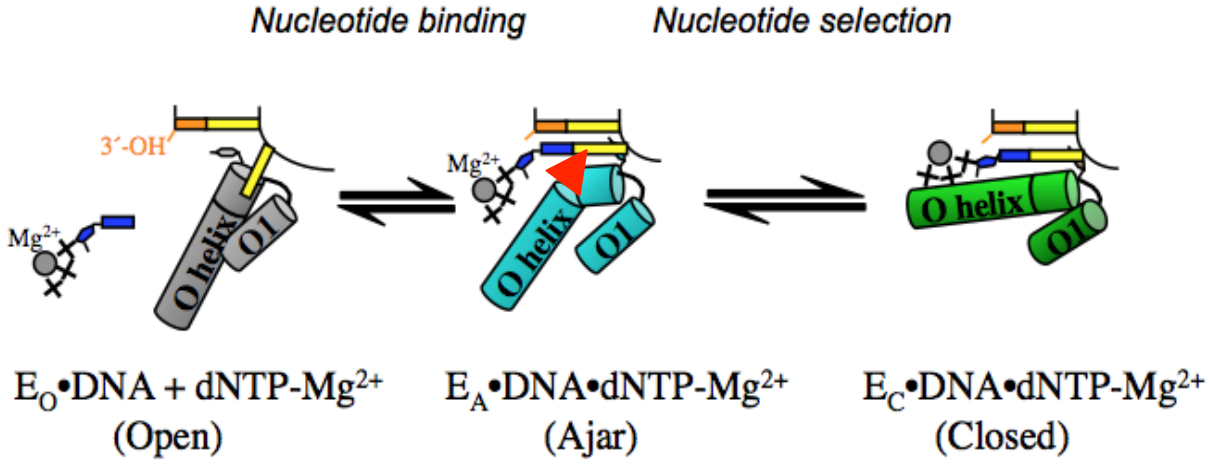

Figure 3.

A-family & homologues (O helix)

BstPolI	699	PNMRRQAKAVNFGIVYGIS	717
EcoPolI	750	SEQRRSAKAINFGLIYGMS	768
TaqPolI	655	PLMRRAAKTINFGVLYGMS	673
hPolG	940	GISREHAKIFNYGRIYGAG	956
hPolQ	1548	DDLRQQAKQICYGIIYGMG	1566
hPolNu	671	HADREQTKKVVYAVVYGAG	689
T7 DNAP	515	LPTRDNAKTFIYGFLYGAG	533
T7 RNAP	615	GVTRSVTKRSVMTLAYGSK	642

Figure 4.

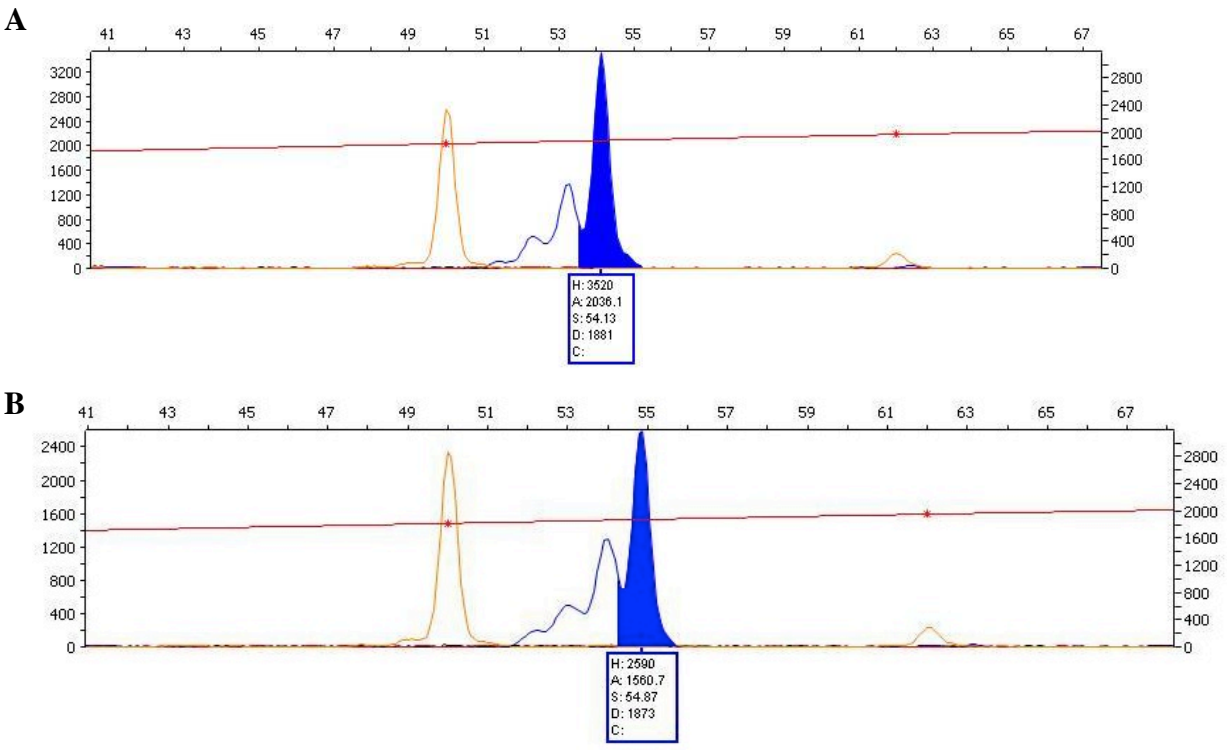

Figure 5.

A

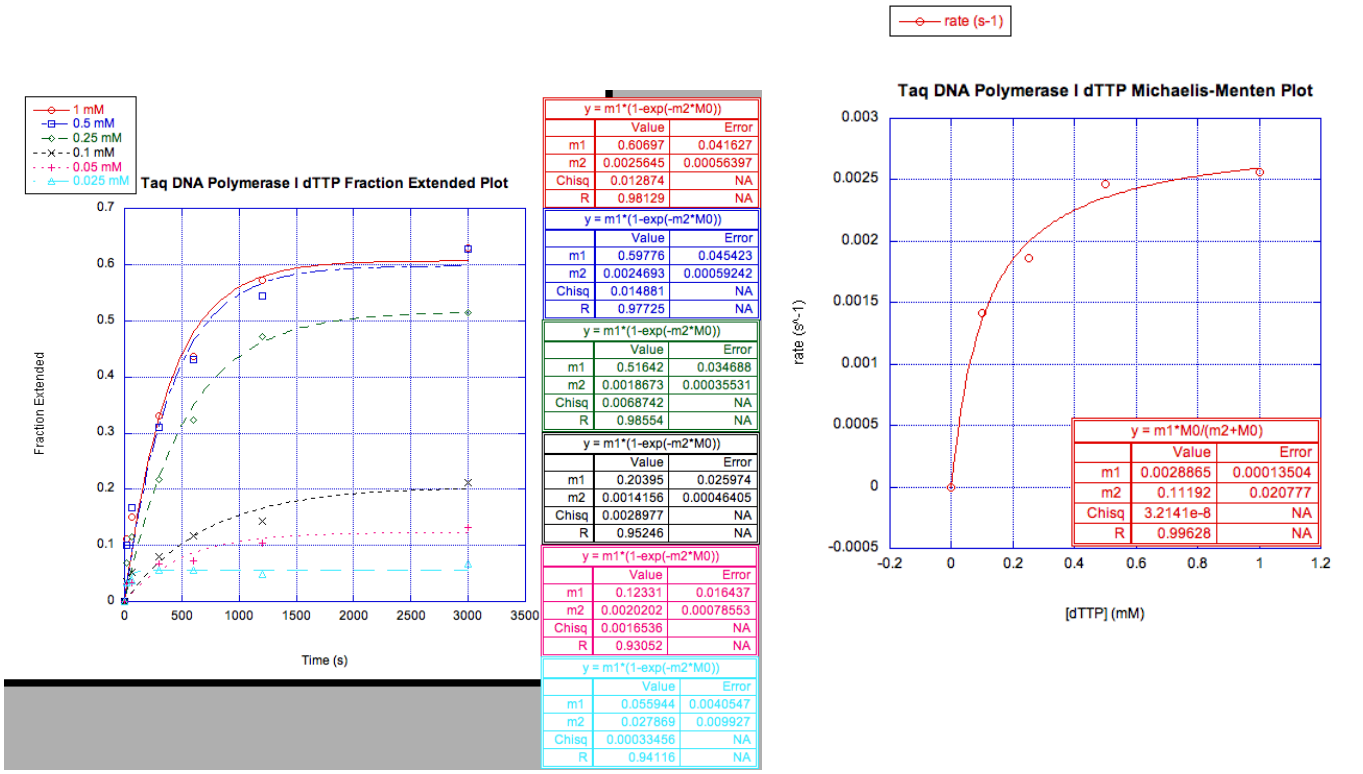
1 mM
0.5 mM
0.25 mM
0.1 mM
0.05 mM
0.025 mM
Taq DNA Polymerase I dTTP Fraction Extended Plot
Fraction Extended
Time (s)
y = m1*(1-exp(-m2*M0))
Value Error
m1 0.60697 0.041627
m2 0.0025645 0.00056397
Chisq 0.012874 NA
R 0.98129 NA
y = m1*(1-exp(-m2*M0))
Value Error
m1 0.59776 0.045423
m2 0.0024693 0.00059242
Chisq 0.014881 NA
R 0.97725 NA
y = m1*(1-exp(-m2*M0))
Value Error
m1 0.51642 0.034688
m2 0.0018673 0.00035531
Chisq 0.0068742 NA
R 0.98554 NA
y = m1*(1-exp(-m2*M0))
Value Error
m1 0.20395 0.025974
m2 0.0014156 0.00046405
Chisq 0.0028977 NA
R 0.95246 NA
y = m1*(1-exp(-m2*M0))
Value Error
m1 0.12331 0.016437
m2 0.0020202 0.00078553
Chisq 0.0016536 NA
R 0.93052 NA
y = m1*(1-exp(-m2*M0))
Value Error
m1 0.055944 0.0040547
m2 0.027869 0.009927
Chisq 0.00033456 NA
R 0.94116 NA
rate (s-1)
Taq DNA Polymerase I dTTP Michaelis-Menten Plot
rate (s^-1)
[dTTP] (mM)
y = m1*M0/(m2+M0)
Value Error
m1 0.0028865 0.00013504
m2 0.11192 0.020777
Chisq 3.2141e-8 NA
R 0.99628 NA

B

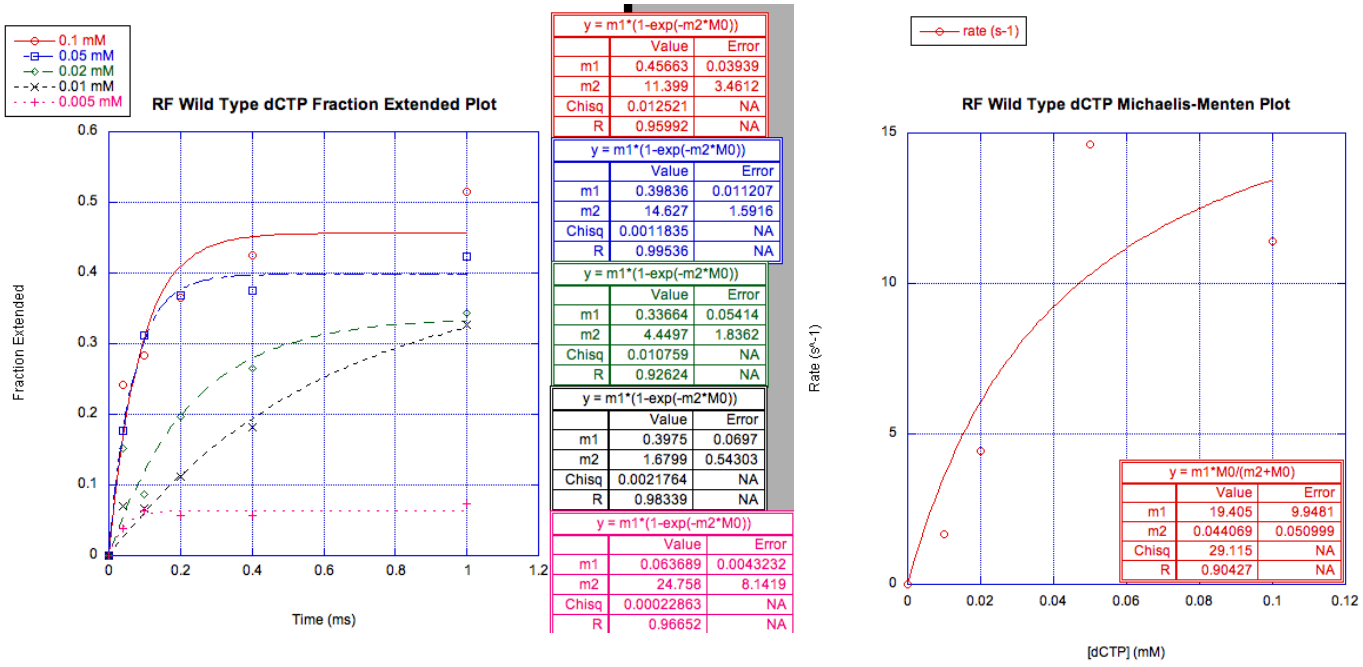
0.1 mM
0.05 mM
0.02 mM
0.01 mM
0.005 mM
RF Wild Type dCTP Fraction Extended Plot
Fraction Extended
Time (ms)
y = m1*(1-exp(-m2*M0))
Value Error
m1 0.45663 0.03939
m2 11.399 3.4612
Chisq 0.012521 NA
R 0.95992 NA
y = m1*(1-exp(-m2*M0))
Value Error
m1 0.39836 0.011207
m2 14.627 1.5916
Chisq 0.0011835 NA
R 0.99536 NA
y = m1*(1-exp(-m2*M0))
Value Error
m1 0.33664 0.05414
m2 4.4497 1.8362
Chisq 0.010759 NA
R 0.92624 NA
y = m1*(1-exp(-m2*M0))
Value Error
m1 0.3975 0.0697
m2 1.6799 0.54303
Chisq 0.0021764 NA
R 0.98339 NA
y = m1*(1-exp(-m2*M0))
Value Error
m1 0.063689 0.0043232
m2 24.758 8.1419
Chisq 0.00022863 NA
R 0.96652 NA
rate (s-1)
RF Wild Type dCTP Michaelis-Menten Plot
Rate (s^-1)
[dCTP] (mM)
y = m1*M0/(m2+M0)
Value Error
m1 19.405 9.9481
m2 0.044069 0.050999
Chisq 29.115 NA
R 0.90427 NA

C

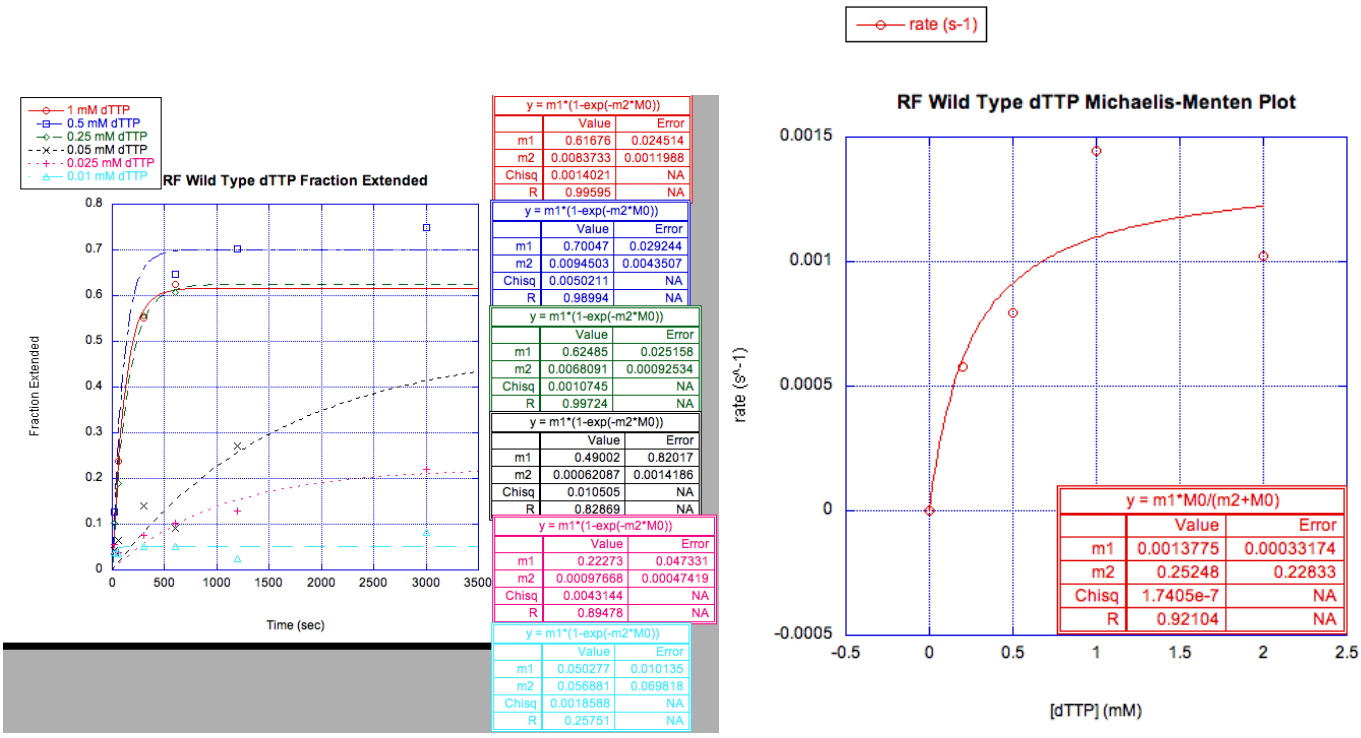
1 mM dTTP
0.5 mM dTTP
0.25 mM dTTP
0.05 mM dTTP
0.025 mM dTTP
0.01 mM dTTP
RF Wild Type dTTP Fraction Extended
Fraction Extended
Time (sec)
y = m1*(1-exp(-m2*M0))
Value Error
m1 0.61676 0.024514
m2 0.0083733 0.0011988
Chisq 0.0014021 NA
R 0.99595 NA
y = m1*(1-exp(-m2*M0))
Value Error
m1 0.70047 0.029244
m2 0.0094503 0.0043507
Chisq 0.0050211 NA
R 0.98994 NA
y = m1*(1-exp(-m2*M0))
Value Error
m1 0.62485 0.025158
m2 0.0068091 0.00092534
Chisq 0.0010745 NA
R 0.99724 NA
y = m1*(1-exp(-m2*M0))
Value Error
m1 0.49002 0.82017
m2 0.00062087 0.0014186
Chisq 0.010505 NA
R 0.82869 NA
y = m1*(1-exp(-m2*M0))
Value Error
m1 0.22273 0.047331
m2 0.00097668 0.00047419
Chisq 0.0043144 NA
R 0.89478 NA
y = m1*(1-exp(-m2*M0))
Value Error
m1 0.050277 0.010135
m2 0.056881 0.069818
Chisq 0.0018588 NA
R 0.25751 NA
rate (s-1)
RF Wild Type dTTP Michaelis-Menten Plot
rate (s^-1)
[dTTP] (mM)
y = m1*M0/(m2+M0)
Value Error
m1 0.0013775 0.00033174
m2 0.25248 0.22833
Chisq 1.7405e-7 NA
R 0.92104 NA

D

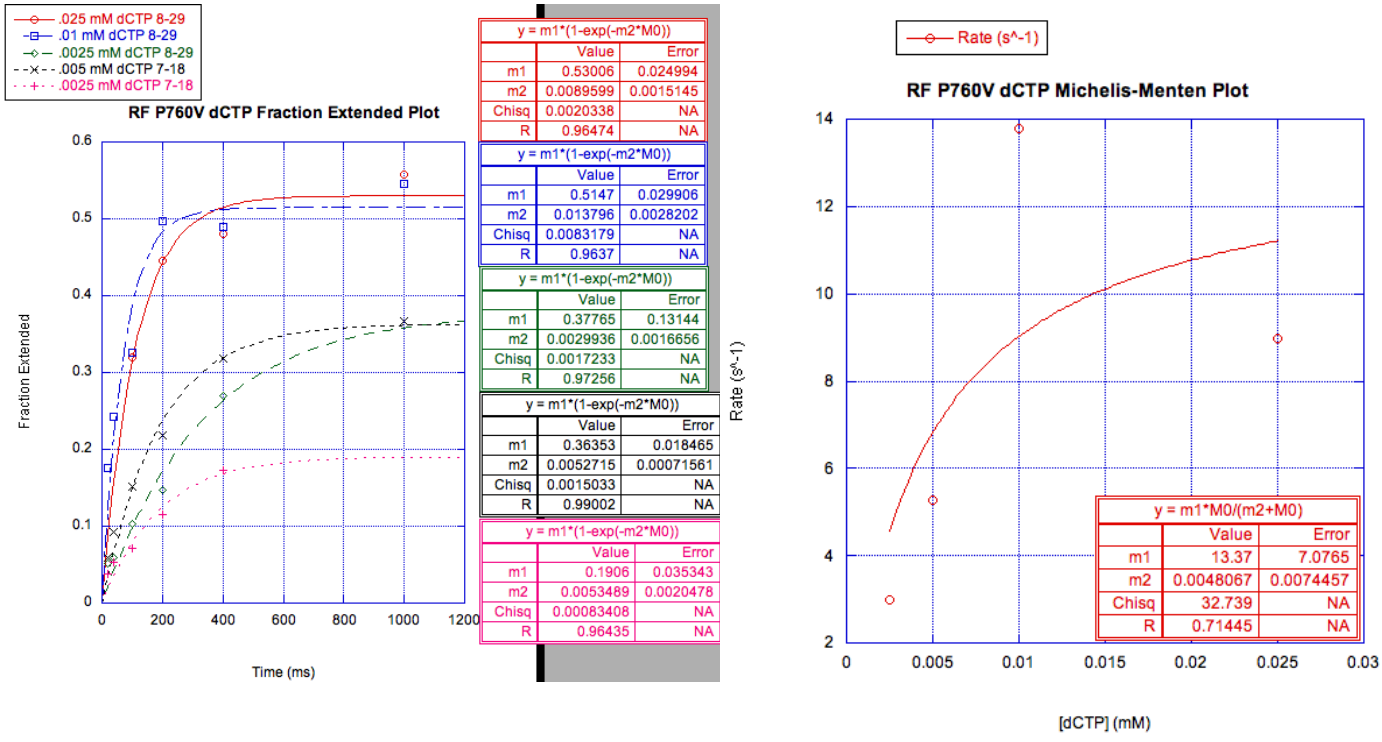
.025 mM dCTP 8-29
.01 mM dCTP 8-29
.0025 mM dCTP 8-29
.005 mM dCTP 7-18
.0025 mM dCTP 7-18
RF P760V dCTP Fraction Extended Plot
Fraction Extended
Time (ms)
y = m1*(1-exp(-m2*M0))
Value Error
m1 0.53006 0.024994
m2 0.0089599 0.0015145
Chisq 0.0020338 NA
R 0.96474 NA
y = m1*(1-exp(-m2*M0))
Value Error
m1 0.5147 0.029906
m2 0.013796 0.0028202
Chisq 0.0083179 NA
R 0.9637 NA
y = m1*(1-exp(-m2*M0))
Value Error
m1 0.37765 0.13144
m2 0.0029936 0.0016656
Chisq 0.0017233 NA
R 0.97256 NA
y = m1*(1-exp(-m2*M0))
Value Error
m1 0.36353 0.018465
m2 0.0052715 0.00071561
Chisq 0.0015033 NA
R 0.99002 NA
y = m1*(1-exp(-m2*M0))
Value Error
m1 0.1906 0.035343
m2 0.0053489 0.0020478
Chisq 0.00083408 NA
R 0.96435 NA
Rate (s^-1)
RF P760V dCTP Michelis-Menten Plot
Rate (s^-1)
[dCTP] (mM)
y = m1*M0/(m2+M0)
Value Error
m1 13.37 7.0765
m2 0.0048067 0.0074457
Chisq 32.739 NA
R 0.71445 NA

E

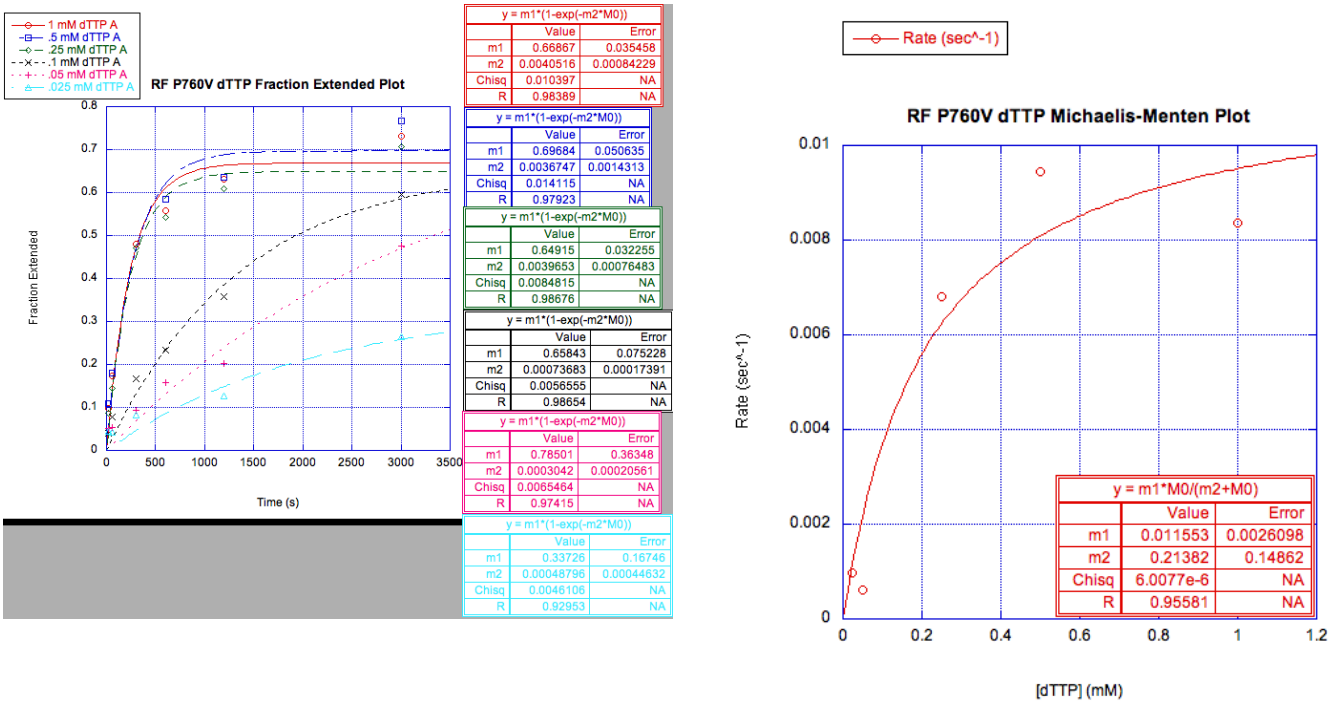

Figure 6.

6-FAM-5’-…58nt-C-3’
3’-…58nt-G-G-5’

Table 1. Pre-steady state kinetic parameters for nucleotide insertion opposite a template guanine in wild-type BF, BF V713P, wild-type RF, RF P760V, and Taq DNA Pol I.

	K_D (μM)	k_{pol} (1/sec)	k_{pol}/K_D (1/M*s)	Relative Efficiency*
Taq DNA Pol I				
dA:dTTP[15]	25.0 ± 3.1	8.80 ± 0.34	352000	1
dG:dTTP	112 ± 21	0.00289 ± 0.00014	25.8	1/13600
BF Wild Type[8]				
dG:dCTP	21	52	2.3	1
dG:dTTP	830	0.55	0.00066	1/3846
BF V713P[8]				
dG:dCTP	12	2.8	0.24	1
dG:dTTP	220	0.0036	0.000017	1/14285
RF Wild Type				
dG:dCTP	44 ± 51	19.4 ± 10	432000	1
dG:dTTP	252 ± 227	0.00137 ± 0.00033	5.4	1/80000
RF P760V				
dG:dCTP	4.8 ± 7.4	13.4 ± 7.1	2792000	1
dG:dTTP	214 ± 149	0.0116 ± 0.0026	54	1/52000

*Relative efficiency is the ratio of k_{pol}/K_D values for dTTP vs dCTP incorporation opposite dG.

References

1. Kunkel TA (2004) DNA replication fidelity. J Biol Chem 279:16895–16898.

2. Joyce CM, Benkovic SJ (2004) DNA polymerase fidelity: kinetics, structure, and checkpoints. Biochemistry 43:14317–14324.

3. Kunkel TA, Bebenek K (2000) DNA replication fidelity. Annu. Rev. Biochem. 69:497–529.

4. Derbyshire V, Freemont PS, Sanderson MR, Beese L, Friedman JM, Joyce CM, Steitz TA (1988) Genetic and crystallographic studies of the 3“,5-”exonucleolytic site of DNA polymerase I. Science 240:199–201.

5. Derbyshire V, Grindley ND, Joyce CM (1991) The 3“-5” exonuclease of DNA polymerase I of Escherichia coli: contribution of each amino acid at the active site to the reaction. EMBO J 10:17–24.

6. Astatke M, Grindley ND, Joyce CM (1998) How E. coli DNA polymerase I (Klenow fragment) distinguishes between deoxy- and dideoxynucleotides. J Mol Biol 278:147–165.

7. Wang W, Wu EY, Hellinga HW, Beese LS (2012) Structural factors that determine selectivity of a high-fidelity DNA polymerase for deoxy-, dideoxy-, and ribo-nucleotides. J Biol Chem.

8. Wu, Eugene Y. and Beese, Lorena S. 2011 The structure of a high fidelity DNA polymerase bound to a mismatched nucleotide reveals an "ajar" intermediate conformation in the nucleotide selection mechanism. Journal of Biological Chemistry Vol. 286, published online March 19, 2011

9. Blondal T, Thorbjarnardottir SH, Kieleczawa J, Hjorleifsdottir S, Kristjansson JK, Einarsson JM, Eggertsson G (2001) Cloning, sequence analysis and functional characterization of DNA polymerase I from the thermophilic eubacterium Rhodothermus marinus. Biotechnol Appl Biochem 34:37–45.

10. Klenow H, Henningsen I (1970) Selective elimination of the exonuclease activity of the deoxyribonucleic acid polymerase from Escherichia coli B by limited proteolysis. Proc. Natl. Acad. Sci. U.S.A. 65:168–175.

11. Setlow P, Brutlag D, Kornberg A (1972) Deoxyribonucleic acid polymerase: two distinct enzymes in one polypeptide. I. A proteolytic fragment containing the polymerase and 3“ leads to 5” exonuclease functions. J Biol Chem 247:224–231.

12. Barnes WM (1992) The fidelity of Taq polymerase catalyzing PCR is improved by an N-terminal deletion. Gene 112:29–35.

13. Kiefer JR, Mao C, Hansen CJ, Basehore SL, Hogrefe HH, Braman JC, Beese LS (1997) Crystal structure of a thermostable Bacillus DNA polymerase I large fragment at 2.1 A resolution. Structure 5:95–108.

14. Chien A, Edgar DB, Trela JM (1976) Deoxyribonucleic acid polymerase from the extreme thermophile Thermus aquaticus. J. Bacteriol. 127:1550–1557.

15. Tindall KR, Kunkel TA (1988) Fidelity of DNA synthesis by the Thermus aquaticus DNA polymerase. Biochemistry 27:6008–6013.

16. Johnson, S.J., Taylor, J.S., and Beese, L.S. (2003) *Proc Natl Acad Sci USA* **100**, 3895-3900.

17. Joyce, C. M., and Benkovic, S. J. (2004) *Biochemistry* **43**, 14317-14324.

18. Johnson S. J., Taylor J. S., Beese L. S. (2003) Processive DNA synthesis observed in a polymerase crystal suggests a mechanism for the prevention of frameshift mutations. Proc. Natl. Acad. Sci. U.S.A. 100, 3895–3900